Title

Covalent Organic Frameworks with Irreversible Linkages via Reductive Cyclization of Imines

Journal

Journal of the American Chemical Society, 144(22)

ISSN

0002-7863

Authors

Yang, Sizhuo
Yang, Chongqing
Dun, Chaochao
et al.

Publication Date

2022-06-08

DOI

10.1021/jacs.2c02405

Peer reviewed

Covalent Organic Frameworks with Irreversible Linkages via Reductive Cyclization of Imines

Sizhuo Yang,[a] Chongqing Yang,[a] Chaochao Dun,[a] Haiyan Mao,[b] Rebecca Shu Hui Khoo,[a] Liana M. Klivansky,[a] Jeffrey A. Reimer,[b,c] Jeffrey J. Urban,[a] Jian Zhang,*[a] and Yi Liu*[a]

[a]The Molecular Foundry, Lawrence Berkeley National Laboratory, Berkeley, California 94720, United States

[b]Department of Chemical and Biomolecular Engineering, University of California, Berkeley, California 94720, United States

[c]Materials Sciences Division, Lawrence Berkeley National Laboratory, Berkeley, California 94720, United States

KEYWORDS. Cadogan reaction, covalent organic frameworks, porous materials, proton conductivity, reductive cyclization

ABSTRACT: Covalent organic frameworks (COFs) show great potential for many advanced applications on account of their structural uniqueness. To address the synthetic challenges, facile chemical routes to engineer porosity, crystallinity and functionality of COFs are highly sought after. Herein we report a synthetic approach that employs the Cadogan reaction to introduce nitrogen-containing heterocycles as the linkage in the framework. Irreversible indazole and benzimidazolylidene (BIY) linkages are introduced into COFs for the first time via phosphine-induced reductive cyclization of the common imine linkages following either stepwise or one-pot reaction protocols. The successful linkage transformation introduces new functionalities, as demonstrated in the case of BIY-COF, which displays excellent

intrinsic proton conductivity without the need of impregnation with external proton transfer reagents. Such a general strategy will open the window to a broader class of functional porous crystalline materials.

INTRODUCTION

As an emerging class of porous crystalline materials, covalent organic frameworks (COFs) are constructed from discrete molecular building blocks through covalent bonds into two dimensional (2D) or three dimensional (3D) extended networks.[1-4] Unlike the classical linear chain polymers, the intrinsic porosity and crystallinity of COFs inherited from structural regularity endow them with superior potentials in gas adsorption,[5] sensing,[6] optoelectronics,[7] and catalysis.[8] Following the basic rules of reticular chemistry,[9-11] the rational design of COFs primarily relies on reversible covalent bonding formation, exemplified by the condensation reactions that furnish boroxines, boronate ester or imines.[12-15] The reversible characters of covalent bonds impart error correction during crystallization,[16] thus preventing the formation of amorphous polymer networks. Such reversibility, however, often diminishes the strength of the covalent linkages. Considerable efforts have been devoted to developing COFs with thermodynamically more stable linkages,[17-18] including vinylene- and dioxin-linked COFs synthesized via Knoevenagel condensation[19-21] and nucleophilic aromatic substitution reactions,[22-24] respectively. Nevertheless, the feasible options to build robust yet reversible linkages are rather limited. An elegant strategy to improve the stability of COFs is to transform the reversible bonds into more robust linkages via postsynthetic modification. Most of the efforts have targeted the C=N bonds in imine-linked COFs, employing oxidation,[25-27] reduction,[28-30] or addition reactions.[31] Despite those demonstrated successes, application of the linkage transformation strategy towards the construction of functional COFs remains largely underexplored. The end products from the imine bond transformation are limited to amides, amines and aromatic ring systems such as quinoline,[31-32] thiazole,[33-34] and oxazole.[35-36] Versatile chemistry that allows for the introduction of new functional units via C=N conversion is thus highly desirable.

To this end, the reduction-induced cyclization involving *o*-nitroaryl imine intermediates, i.e. the Cadogan reaction, appears to be an excellent choice.[37-38] In fact, Cadogan reaction has been widely adopted for the synthesis of nitrogen-containing aromatics.[39] As illustrated in Scheme 1a, indazoles can be readily obtained from the reaction between *o*-nitrobenzaldehyde and arylamine, which firstly generates an imine intermediate, followed by an intramolecular reductive cyclization initiated by a trivalent phosphine reagent.[38] The resulting COFs may inherit the biological activities of indazole linkage, such as antitumor, anticancer, antimicrobial, antidepressant and HIV-protease inhibition activities,[40-43] thus inspire potential applications in medicinal chemistry. In a similar fashion benzimidazoles can be obtained (Scheme 1b).[44] In both cases, reduction of an auxiliary nitro group by a phosphine reagent induces the transformation of aryl imine into heterocyclic aromatics with high fidelity. In this work, combining the dynamic imine chemistry and the Cadogan reaction, we have successfully synthesized an indazole-linked COF via both one-pot reaction and postsynthetic modification. In addition, this strategy imbued the discovery of a novel benzimidazolylidene (BIY)-linked COFs. The potential utility of this synthetic strategy was further highlighted by the excellent proton conductivity of the BIY-linked COF.

Scheme 1. Formation of a) indazole and b) benzimidazole via Cadogan reaction that involves cascade condensation and reductive cyclization

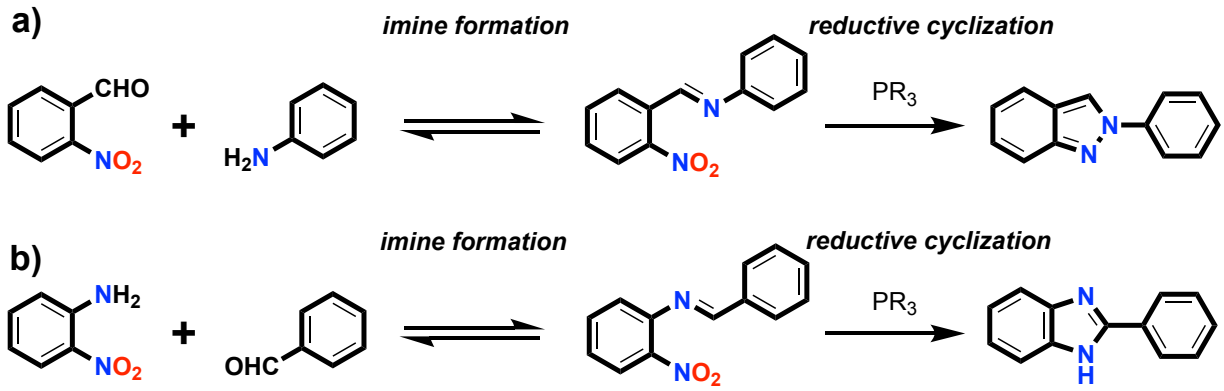

RESULTS AND DISCUSSION

Synthesis of Indazole-Linked COF. The effectiveness of the Cadogan reaction for COF synthesis was initially investigated by a stepwise protocol involving the reaction between dinitro-substituted 4,4′-biphenyldicarboxaldehyde (**1**) (Figure S1-S2) and 1,3,5-tris(4-aminophenyl)benzene (TPB, **2**) (Scheme 2). TPB-imine-COF was obtained under conventional solvothermal conditions using a mixture of mesitylene and dioxane (5.6:1, v/v) with acetic acid (8 M) as the catalyst (120 °C, 3 days). After washing with organic solvents and vacuum drying, the obtained TPB-imine-COF was subjected to reacting with P(*n*-Bu)$_3$ in *o*-dichlorobenzene (ODCB) at 110 °C for 6 hours, which successfully produced the desired TPB-indazole-COF.

Scheme 2. Synthesis of TPB-indazole-COF via stepwise or one-pot approaches. ODCB: *o*-dichlorobenzene

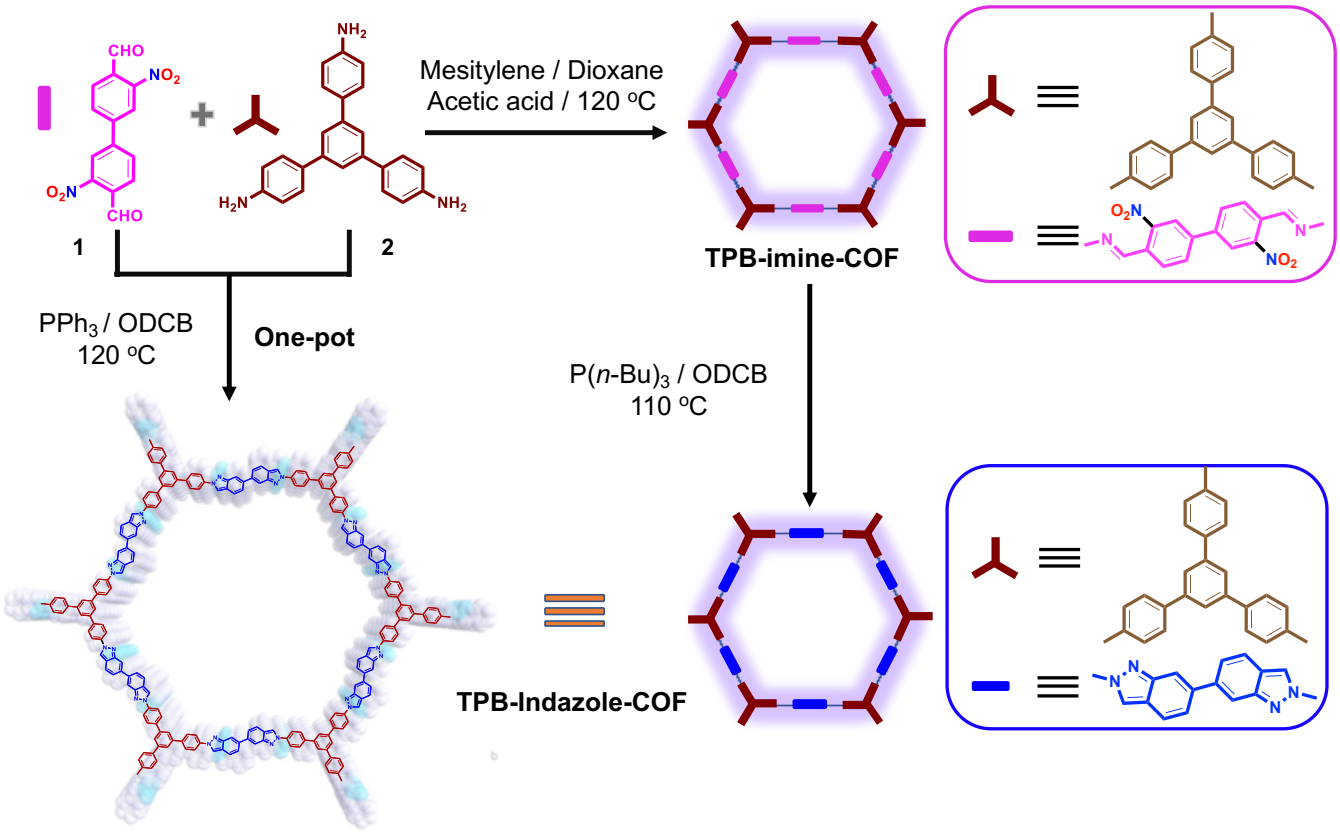

The crystallinity of TPB-imine-COF and TPB-indazole-COF was verified by powder X-ray diffraction (PXRD) studies. The PXRD pattern of TPB-imine-COF exhibits prominent peaks at 2.25°, 3.95°, 4.60°, 6.17°, 7.99° and 25.15°, which can be assigned to the (100), (110), (200), (210), (220) and (001) facets, respectively (Figure S12). TPB-indazole-COF displays similar diffraction patterns (Figure 1a), with the most intense peak at 2.46° and other peaks at 4.13° and 25.21°, corresponding to the (100), (110) and (001) facets, respectively. Pawley refined patterns of the simulated structures of both COFs in their eclipsed stacking modes agree well with the experimental results, as indicated by the negligible difference spectra (Figure 1a and Figure S11). The TPB-imine-COF was assigned to the space group *P*6/*m* with optimized cell parameters of α=β=90°, γ=120°, a=b=45.56 Å, c=3.54 Å. The same space group was assigned to TPB-indazole-COF with a slightly different set of cell parameters of α=β=90°, γ=120°, a=b=42.94 Å, c=3.44 Å (Table S1), supporting that the framework structure was retained after linkage transformation.

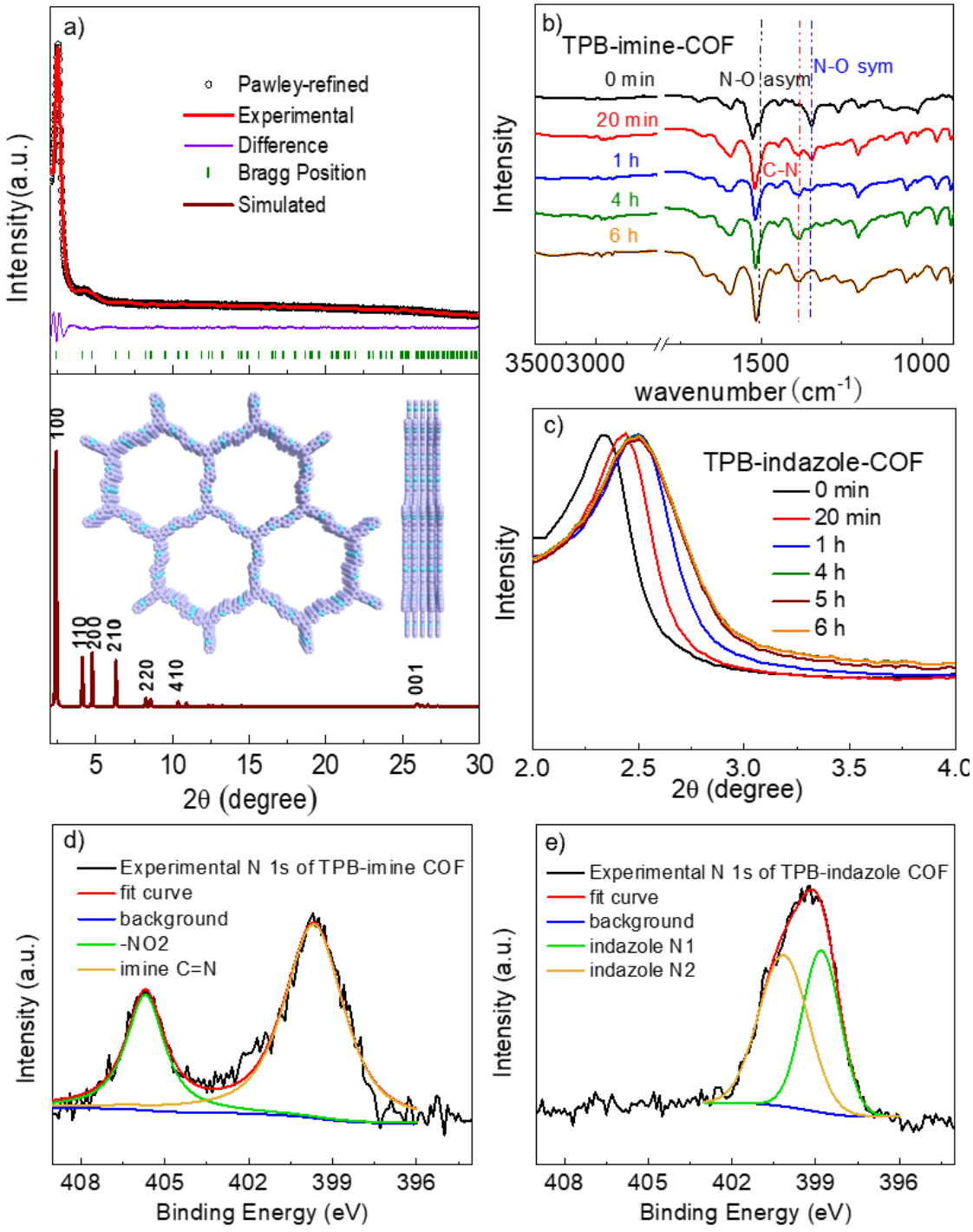

Figure 1. a) Experimental and simulated PXRD patterns of TPB-indazole-COF, together with the Pawley-refined and the difference spectra. Time-lapse b) FT-IR and c) PXRD changes of TPB-imine-COF upon reduction, showing the formation of TPB-indazole COF. XPS spectra of d) TPB-imine-COF and e) TPB-indazole-COF.

Fourier transform infrared (FT-IR) spectroscopic studies further supported the successful chemical transformation. The FT-IR spectrum of TPB-imine-COF shows the characteristic C=N stretching mode at 1620 cm^{-1} and the absence of amino (3200-3500 cm^{-1}) and aldehyde vibrations (1663-1730 cm^{-1}), consistent with the formation of the imine-linked framework (Figure S13a). In comparison, the FT-IR spectrum of TPB-indazole-COF reveals the disappearance of both the imine vibration at 1620 cm^{-1} and the N-O symmetric (1340 cm^{-1}) and asymmetric stretches (1525 cm^{-1}), accompanied by the appearance of the indazole C-N stretching at 1380 cm^{-1} (Figure 1b and S13b). Moreover, the TPB-indazole-COF exhibits almost identical vibrational stretching modes to its corresponding indazole model compound (**M1**) that was synthesized separately by either stepwise condensation-reductive cyclization reactions or the one-pot Cadogan reaction (Scheme S2, Figure S3-S7, and Figure S13b). Those together indicated the reduction of nitro groups and the subsequent cyclization to give the indazole-linked COF in very high yield.

Time-lapse PXRD and FT-IR studies revealed further evidence of the structural transformation during the reductive cyclization. As shown in Figure 1c, the (100) facet of TPB-imine-COF undergoes a progressive shift from 2.25° to 2.46° within 4 hours, indicating a gradual lattice shrinkage as TPB-imine-COF transforms to TPB-indazole-COF. Such changes corroborated with the FT-IR spectra which revealed monotonically diminishing NO_2 vibrations over time (Figure 1b). No NO_2 peaks were observed after 6 hours, confirming the complete imine-to-indazole conversion.

The successful conversion was cross-verified by X-ray photoelectron spectroscopy (XPS). The *N* 1s signals at ~405 eV and ~398 eV in the XPS spectrum of TPB-imine-COF (Figure 1d) are ascribable to the NO_2 and C=N moieties, respectively. Upon reductive cyclization, a new shoulder peak at ~401 eV associated with indazole *N* atoms was observed while the nitro signal disappeared completely (Figure 1e), indicating the full cyclization of imine and nitro groups and the formation of indazoles. The C 1s spectra showed signals from sp^2 C and sp^3 C for both TPB-imine-COF and TPB-indazole-COF, consistent with the expected structures (Figure S16). Solid-state ^{13}C cross-polarization magic angle spinning (CP-MAS)

NMR spectra of the COFs are also consistent with such functional group transformations (Figure S14a). Both COFs possess permanent porosity and exhibit a type IV isotherm, as measured by N_2 sorption experiments at 77 K (Figure S15). The Brunauer-Emmett-Teller (BET) surface areas of the TPB-imine- and TPB-indazole-COF were calculated to be 808 m^2/g and 617 m^2/g, and the pore size distributions simulated by nonlocal density functional theory (NLDFT) showed average pore sizes of 3.49 nm and 3.04 nm, respectively (FigureS15, inset). Scanning electron microscopy (SEM) revealed spherical morphologies for both COFs (Figure S18). Diffuse reflectance UV−visible spectrum of TPB-indazole-COF exhibits an extended absorption towards the longer wavelength (~550 nm), corresponding to a reduced optical band gap of 2.32 eV that results from the extended π conjugation in the indazole framework (Figure S19). The chemical stability of TPB-indazole-COF was tested by immersing the materials in different solvents. The crystallinity retains after soaking in DMF and H2O for 1 week. TPB-indazole-COF also exhibits good stability in acid: only a slight broadening of the (100) peak was observed after soaking in HCl (9 M) for 7 days. However, it is less stable in base and the decrease of crystallinity was more pronounced after soaking in a NaOH (10 M) solution for 3 days (Figure S20). The susceptibility to strong acidic and basic conditions presumably stems from the low chemical stability of the indazole unit, as indicated by the ^{1}H NMR results of **M1** under acidic and basic conditions (Figure S21).

TPB-indazole-COF could also be obtained using a one-pot method, attesting to the versatility of the Cadogan approach. When heating **1**, **2** and PPh_3 in a mixture of dioxane and mesitylene at 120 °C for 3 days, the desired TPB-indazole-COF was obtained, despite a slightly lower crystallinity compared to the COF obtained from the stepwise synthesis (Figure S22).

Synthesis of BIY-Linked COF: The successful synthesis of the indazole-linked COF using Cadogan reaction encouraged us to extend this methodology to COFs with other heterocyclic linkages, such as the benzimidazole unit. We employed the divalent 3,3'-dinitro-benzidine (**4**) and the trivalent 2,4,6-trimethoxybenzene-1,3,5-tricarbaldehyde (**3**) as the precursors (Scheme 3b). We first attempted the stepwise approach and, to our surprise, the solvothermal condensation reaction led to the spontaneous

demethylation of the condensation product, as revealed by the solid-state NMR spectrum (Figure S14b) which matched well with a β-ketoenamine-linked COF.[45] Presumably following the demethylation, the thus generated enol-imine form COF undergoes the well-known irreversible enol-keto tautomerization to give the COF product in the β-ketoenamine form as Ketoenamine-NO_2-COF shown in Scheme 3b. This result contrasts the previously reported structure which assumed an imine form with full preservation of the methyl groups.[46] Ketoenamine-NO_2-COF did not undergo the subsequent reductive cyclization and failed to yield the desired benzimidazole COF.

We then turned to the one-pot route, envisioning that the reductive environment would promote *in situ* cyclization of the imine intermediate preceding the tautomerization. The feasibility of this transformation was firstly verified by a model reaction that involved heating **3**, *o*-nitroaniline and P(*n*-Bu)$_3$ in ODCB. Interestingly, the product **M2** was obtained as a tribenzimidazolylidene trisketone, the solid-state structure of which was confirmed by single crystal X-ray diffraction study (Scheme 3a). Both mass spectrum and NMR spectra of **M2** were fully consistent with a highly symmetric ketone species with no methyl groups (Figure S8-S10). The effective synthesis of **M2** verifies that following the formation of imines, the reductive cyclization readily occurs in the presence of P(*n*-Bu)$_3$ and outcompetes demethylation, furnishing the transformation of imines into benzimidazoles. Demethylation and tautomerization nevertheless occur after cyclization, in a fashion similar to that observed in the formation of Ketoenamine-NO_2-COF.

Scheme 3. a) Illustration of the formation of **M2** from the model Cadogan reaction. The X-ray structure supports demethylation and tautomerization steps following the successful reductive cyclization. b) Synthesis of BIY-COF: successful one-pot approach vs ineffective stepwise route.

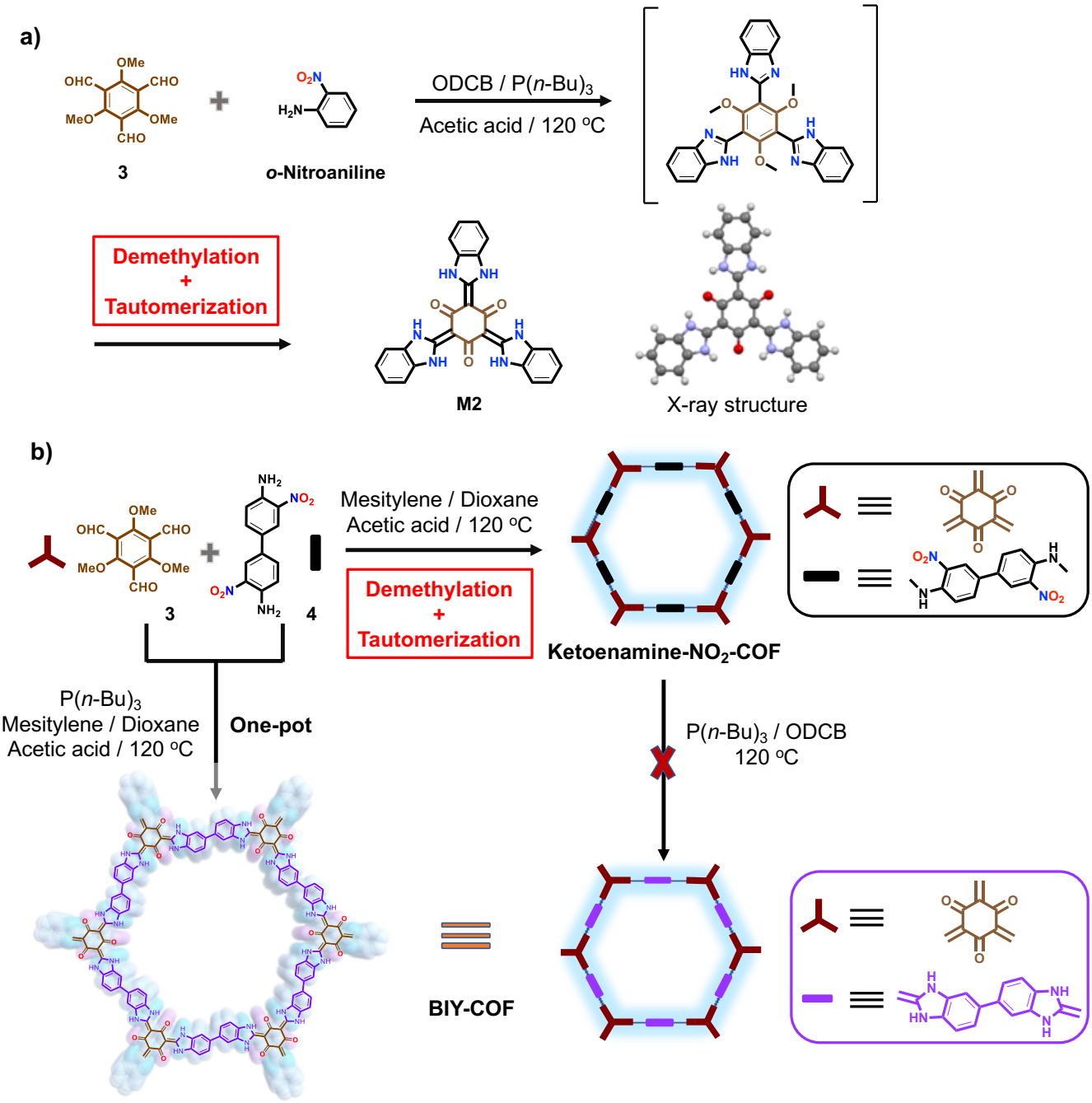

The successful reductive cyclization encouraged us to proceed with the one-pot Cadogan COF synthesis, which generated the corresponding BIY-COF (Scheme 3b). The structure of BIY-COF was supported by various spectroscopic studies. Comparing the FT-IR spectrum of BIY-COF against that of the Ketoenamine-NO_2-COF revealed the disappearance of the N-O symmetric (1340 cm^{-1}) and asymmetric stretches (1525 cm^{-1}) (Figure 2a). Furthermore, the C=C vibration peak at 1552 cm^{-1} in the

FT-IR spectrum of BIY-COF was similar to that in the spectrum of model compound **M2**, but distinct from that of the Ketoenamine-NO_2-COF which appeared at 1572 cm^{-1} (Figure 2a). The formation of BIY linkage was also evidenced by comparing the XPS of BIY-COF and Ketoenamine-NO_2-COF (Figure 2b and Figure S17). The *N* 1s signal at 405 eV in the XPS of Ketoenamine-NO_2-COF, corresponding to nitro groups, disappeared in that of BIY-COF. A major *N* 1s peak at 400 eV was attributed to the BIY *N* atoms, while the shoulder at 398 eV may suggest the presence of small percentage of tautomeric benzimidazole ring system. ^{13}C CP-MAS NMR spectroscopy revealed the disappearance of methyl carbon resonance, along with the resonances from the expected aromatic core (Figure S14b).

The PXRD of BIY-COF displays a series of prominent peaks, with the most intense one at 3.46 ° and other peaks at 5.34 °, 9.65 ° and 26.04 °, corresponding to the (100), (110), (210) and (001) facets, respectively (Figure 2c). The experimental PXRD pattern agrees well with the simulation based on the eclipsed stacking mode (inset in Figure 2c). Pawley refinement of the simulated structure with the P6/m space group yields the optimized cell parameters of α=β=90°, γ=120°, a=b=28.41 Å, c=3.44 Å. The permanent porosity of BIY-COF was confirmed by N_2 sorption measurements at 77 K, with a BET surface area of 1023 m^2/g (Figure S15). The SEM image of BIY-COF exhibits a fibrillar morphology with a width of 80 nm, which forms flower-like aggregates with a diameter of approximately 2 μm (Figure S18). Unlike TPB-indazole-COF, the BIY-COF shows excellent chemical stability, as indicated by the negligible change in position and intensity of XRD patterns after its dispersion in DMF, H_2O, HCl (9 M), H_2SO_4 (9 M in DMSO) and NaOH (10 M) solutions for 1 week (Figure S20b).

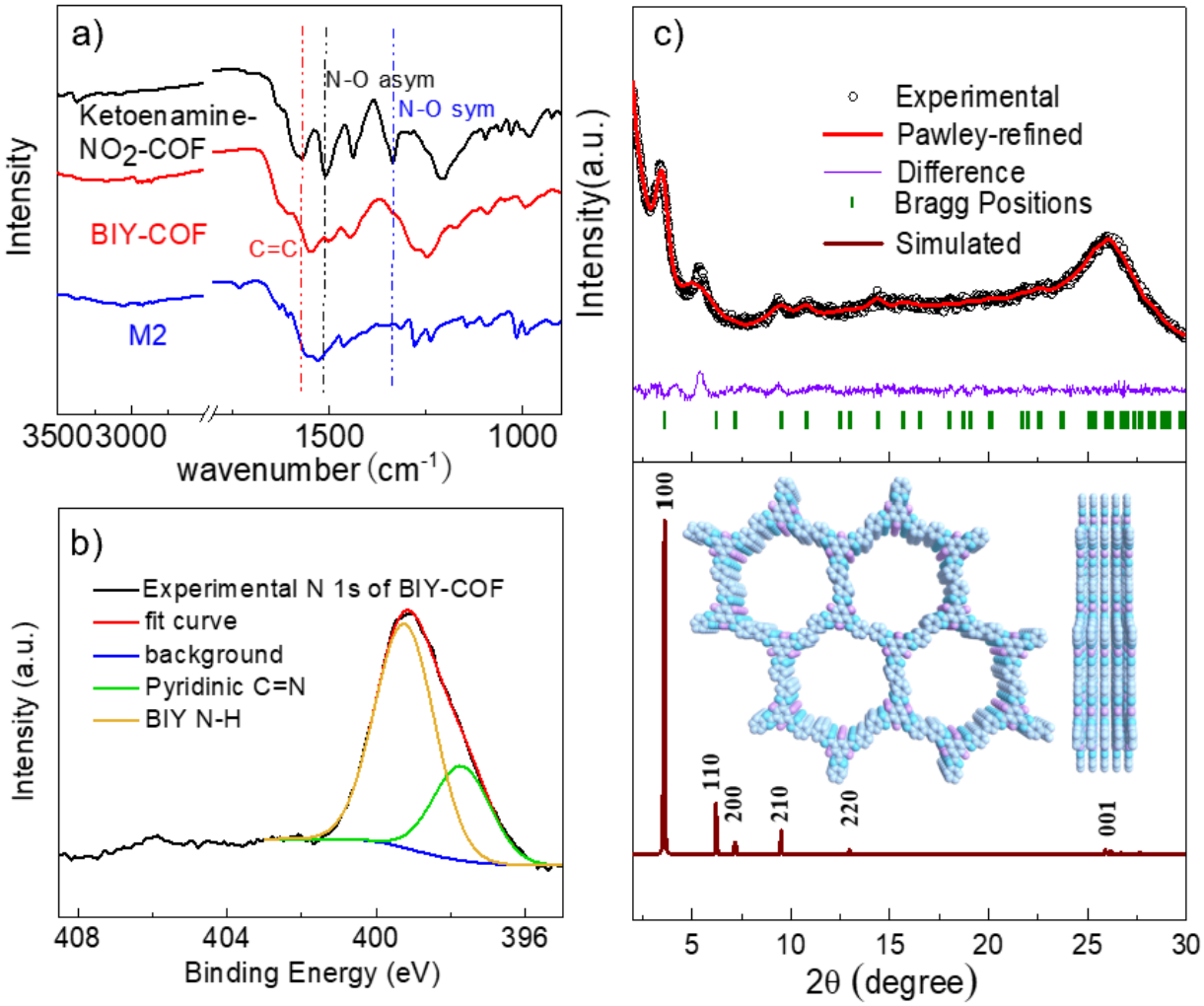

Figure 2. a) FT-IR of BIY-COF, Ketoenamine-NO_2-COF and the model compound **M2**. b) XPS of BIY-COF. c) Experimental and simulated PXRD of BIY-COF, together with the Pawley-refined and the difference spectra.

Proton Transport Properties. COF-based proton conductive materials have recently received growing interest for their high surface areas and well defined pore sizes.[47] Most of the reported examples are obtained by compositing a COF matrix with external proton transfer reagents.[48-51] Few COFs have demonstrated intrinsic proton conductivity due to the lack of proton transfer moieties within the framework. Babu et al. is amongst the first to incorporate proton conductive benzimidazole units into a

COF that displayed high intrinsic proton conductivity.[52-53] The new BIY-COF showcases a high density of ketones and BIY moieties that could act as proton acceptor and donors, respectively, alluding to its great potential as an intrinsic proton transfer material with high conductivity.

To study the proton conduction of BIY-COF, electrochemical impedance spectroscopy (EIS) was carried out using compressed pellets under controlled humid environment. BIY-COF exhibit almost negligible proton conductivity at 35 °C under anhydrous conditions, as indicated by the noisy Nyquist plot (Figure S23). In contrast, the proton conductivity dramatically increases under humid conditions (Figure S24, 7.4×10^{-3} S/cm at 35 °C, 95% relative humidity, RH), indicating that water plays a significant role in proton transfer. The conductivity of BIY-COF increases with temperature and reaches a maximum value of 1.9×10^{-2} S/cm (95 °C, 95% RH) (Figure 3a), which is comparable to the highest values of the reported COFs with intrinsic proton conductivity (entry 6 and 11 in Table S4) and outperforms many COFs impregnated with extrinsic proton conductors. The excellent performance can be attributed to the formation of a stable proton network through the 1D channel formed by aligned pores, thanks to the proton donating and accepting characters of the new BIY unit. For comparison, we also measured the proton conductivity of Ketoenamine-NO_2-COF at different temperatures It shows a much lower proton conductivity of 1.95×10^{-5} S/cm at 95 °C and 95% RH (Figure S25), due to the absence of benzimidazole and/or hydroxyl groups. EIS measurements were also carried out for TPB-indazole-COF and TPB-imine-COF at different temperatures, revealing proton conductivity values of 4.59×10^{-6} S/cm and 3.41×10^{-7} S/cm at 95 °C and 95% RH (Figure 3b and S25), respectively. The superior performance of BIY-COF highlights the crucial contributions of the proton donor and acceptor moieties to the COF's intrinsic proton conductivity. BIY-COF and TPB-indazole-COF were subjected to further EIS studies at different temperatures, from which activation energy (E_a) were obtained. From their Arrhenius plots, E_a of BIY-COF and TPB-indazole-COF were determined to be 0.24 eV and 0.33 eV (Figure 3c, d), respectively, revealing the Grotthuss-type proton transfer mechanism in both COFs where protons "hop" along the proton network through the wall of the framework.[51, 54-55] The stability of both COFs under the EIS

conditions was confirmed by XRD and FT-IR studies (Figure S26 and S27), which revealed negligible differences before and after the measurement.

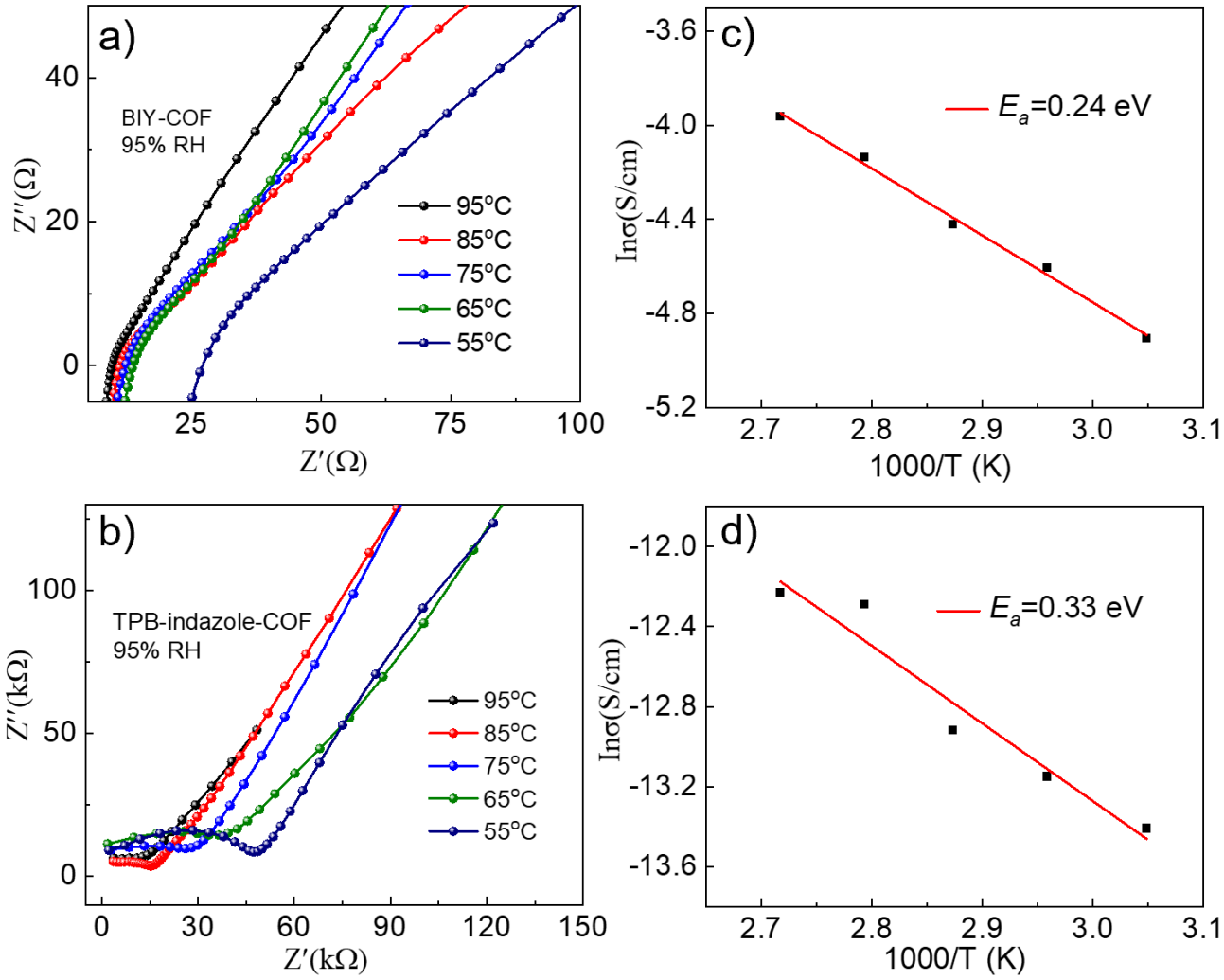

Figure 3. Proton conductivity measurement. Nyquist plots of a) BIY-COF and b) TPB-indazole-COF at different temperature (95% RH). Arrhenius plot for c) BIY-COF and d) TPB-indazole-COF.

CONCLUSION

We have developed a new synthetic strategy that employs Cadogan reaction to introduce nitrogen-containing heterocyclic units as both linkages and functional units in hitherto unreported COFs. As a proof of concept, indazole and BIY-linked COFs have been synthesized either stepwise or one-pot, via the

formation of nitro-containing imine intermediates and phosphine-induced reductive cyclization. This method offers versatile options to construct COFs with irreversible heterocyclic linkages via reversible imine bonds and presents conceivable opportunities to control COF's band gap and other semiconducting properties. Taking advantage of the functionality of the Cadogan product, such as the excellent proton transfer properties of BIY, we have demonstrated the utility of this strategy in synthesizing COFs with excellent intrinsic proton conductivity. Future efforts in combining the Cadogan reaction motif with the reticular chemistry of COFs will open the door to a broader class of functional porous crystalline materials.

ASSOCIATED CONTENT

Supporting Information. The Supporting Information is available free of charge at http://pubs.acs.org. Details of synthetic procedures, solution and solid-state NMR spectra, N_2 adsorption and desorption isotherms, proton conductivity measurement, structure simulation, FT-IR spectra.

Accession Codes. CCDC 2155577 contains the supplementary crystallographic data for this paper. These data can be obtained free of charge via www.ccdc.cam.ac.uk/data_request/cif, or by emailing data_request@ccdc.cam.ac.uk, or by contacting The Cambridge Crystallographic Data Centre, 12 Union Road, Cambridge CB2 1EZ, UK; fax: +44 1223 336033.

AUTHOR INFORMATION

Corresponding Authors

Yi Liu–The Molecular Foundry, Lawrence Berkeley National Laboratory, Berkeley, California 94720, United States; Email: yliu@lbl.gov

Jian Zhang–The Molecular Foundry, Lawrence Berkeley National Laboratory, Berkeley, California 94720, United States; Email: jianzhang@lbl.gov

Authors

Sizhuo Yang- The Molecular Foundry, Lawrence Berkeley National Laboratory, Berkeley, California 94720, United States; Email: sizhuoyang@lbl.gov

Chongqing Yang- The Molecular Foundry, Lawrence Berkeley National Laboratory, Berkeley, California 94720, United States; Email: chongqing@lbl.gov

Chaochao Dun- The Molecular Foundry, Lawrence Berkeley National Laboratory, Berkeley, California 94720, United States; Email: cdun@lbl.gov

Haiyan Mao- Department of Chemical and Biomolecular Engineering, University of California, Berkeley, California 94720, United States; Email: maohaiyan@berkeley.edu

Rebecca Shu Hui Khoo- The Molecular Foundry, Lawrence Berkeley National Laboratory, Berkeley, California 94720, United States; Email: rkhoo@lbl.gov

Liana M. Klivansky- The Molecular Foundry, Lawrence Berkeley National Laboratory, Berkeley, California 94720, United States; Email: lmklivansky@lbl.gov

Jeffrey A. Reimer- Department of Chemical and Biomolecular Engineering, University of California, Berkeley, California 94720, United States; Email: reimer@berkeley.edu

Jeffrey J. Urban- The Molecular Foundry, Lawrence Berkeley National Laboratory, Berkeley, California 94720, United States; Email: jjurban@lbl.gov

Notes

The authors declare no competing financial interest.

ACKNOWLEDGMENT

Work at the Molecular Foundry was supported by the Office of Science, Office of Basic Energy Sciences, of the U.S. Department of Energy under Contract No. DE-AC02-05CH11231. H.M. and J.A.R.

acknowledge partial support from Department of Energy (DOE), Office of Basic Energy Sciences, Division of Materials Sciences and Engineering (Contract No. DE-AC02-76SF00515). We thank Dr. Hasan Celik, and the College of Chemistry NMR Facility, University of California, Berkeley.

REFERENCES

1. Côté, A. P.; Benin, A. I.; Ockwig, N. W.; O'Keeffe, M.; Matzger, A. J.; Yaghi, O. M., Porous, Crystalline, Covalent Organic Frameworks. *Science* **2005**, *310*, 1166-1170.
2. Diercks, C. S.; Yaghi, O. M., The atom, the molecule, and the covalent organic framework. *Science* **2017**, *355*, 923-931.
3. Feng, X.; Ding, X. S.; Jiang, D. L., Covalent organic frameworks. *Chem. Soc. Rev.* **2012**, *41*, 6010-6022.
4. Gui, B.; Lin, G.; Ding, H.; Gao, C.; Mal, A.; Wang, C., Three-Dimensional Covalent Organic Frameworks: From Topology Design to Applications. *Acc. Chem. Res.* **2020**, *53*, 2225-2234.
5. Huang, N.; Chen, X.; Krishna, R.; Jiang, D., Two-Dimensional Covalent Organic Frameworks for Carbon Dioxide Capture through Channel-Wall Functionalization. *Angew. Chem. Int. Ed.* **2015**, *54*, 2986-2990.
6. Song, Y.; Sun, Q.; Aguila, B.; Ma, S., Opportunities of Covalent Organic Frameworks for Advanced Applications. *Adv. Sci.* **2019**, *6*, 1801410.
7. Keller, N.; Bein, T., Optoelectronic processes in covalent organic frameworks. *Chem. Soc. Rev.* **2021**, *50*, 1813-1845.
8. Hasija, V.; Patial, S.; Raizada, P.; Khan, A. A. P.; Asiri, A. M.; Le, Q. V.; Nguyen, V. H.; Singh, P., Covalent organic frameworks promoted single metal atom catalysis: Strategies and applications. *Coord. Chem. Rev.* **2022**, *452*, 214298.
9. Ding, S. Y.; Wang, W., Covalent organic frameworks (COFs): from design to applications. *Chem. Soc. Rev.* **2013**, *42*, 548-568.
10. Geng, K. Y.; He, T.; Liu, R. Y.; Dalapati, S.; Tan, K. T.; Li, Z. P.; Tao, S. S.; Gong, Y. F.; Jiang, Q. H.; Jiang, D. L., Covalent Organic Frameworks: Design, Synthesis, and Functions. *Chem. Rev.* **2020**, *120*, 8814-8933.
11. Freund, R.; Canossa, S.; Cohen, S. M.; Yan, W.; Deng, H. X.; Guillerm, V.; Eddaoudi, M.; Madden, D. G.; Fairen-Jimenez, D.; Lyu, H.; Macreadie, L. K.; Ji, Z.; Zhang, Y. Y.; Wang, B.; Haase, F.; Woll, C.; Zaremba, O.; Andreo, J.; Wuttke, S.; Diercks, C. S., 25 Years of Reticular Chemistry. *Angew. Chem. Int. Ed.* **2021**, *60*, 23946-23974.
12. Segura, J. L.; Mancheno, M. J.; Zamora, F., Covalent organic frameworks based on Schiff-base chemistry: synthesis, properties and potential applications. *Chem. Soc. Rev.* **2016**, *45*, 5635-5671.
13. Waller, P. J.; Gándara, F.; Yaghi, O. M., Chemistry of Covalent Organic Frameworks. *Acc. Chem. Res.* **2015**, *48*, 3053-3063.
14. Lanni, L. M.; Tilford, R. W.; Bharathy, M.; Lavigne, J. J., Enhanced Hydrolytic Stability of Self-Assembling Alkylated Two-Dimensional Covalent Organic Frameworks. *J. Am. Chem. Soc.* **2011**, *133*, 13975-13983.
15. Zhan, G. L.; Cai, Z. F.; Martinez-Abadia, M.; Mateo-Alonso, A.; De Feyter, S., Real-Time Molecular-Scale Imaging of Dynamic Network Switching between Covalent Organic Frameworks. *J. Am. Chem. Soc.* **2020**, *142*, 5964-5968.

16. Smith, B. J.; Dichtel, W. R., Mechanistic Studies of Two-Dimensional Covalent Organic Frameworks Rapidly Polymerized from Initially Homogenous Conditions. *J. Am. Chem. Soc.* **2014**, *136*, 8783-8789.
17. Li, X. L.; Cai, S. L.; Sun, B.; Yang, C. Q.; Zhang, J.; Liu, Y., Chemically Robust Covalent Organic Frameworks: Progress and Perspective. *Matter* **2020**, *3*, 1507-1540.
18. Li, X. L.; Wang, H. X.; Chen, H.; Zheng, Q.; Zhang, Q. B.; Mao, H. Y.; Liu, Y. W.; Cai, S. L.; Sun, B.; Dun, C. C.; Gordon, M. P.; Zheng, H. M.; Reimer, J. A.; Urban, J. J.; Ciston, J.; Tan, T. W.; Chan, E. M.; Zhang, J.; Liu, Y., Dynamic Covalent Synthesis of Crystalline Porous Graphitic Frameworks. *Chem* **2020**, *6*, 933-944.
19. Jin, E.; Asada, M.; Xu, Q.; Dalapati, S.; Addicoat, M. A.; Brady, M. A.; Xu, H.; Nakamura, T.; Heine, T.; Chen, Q.; Jiang, D., Two-dimensional sp 2 carbon-conjugated covalent organic frameworks. *Science* **2017**, *357*, 673-676.
20. Bi, S.; Thiruvengadam, P.; Wei, S.; Zhang, W.; Zhang, F.; Gao, L.; Xu, J.; Wu, D.; Chen, J.-S.; Zhang, F., Vinylene-Bridged Two-Dimensional Covalent Organic Frameworks via Knoevenagel Condensation of Tricyanomesitylene. *J. Am. Chem. Soc.* **2020**, *142*, 11893-11900.
21. Yang, S.; Streater, D.; Fiankor, C.; Zhang, J.; Huang, J., Conjugation- and Aggregation-Directed Design of Covalent Organic Frameworks as White-Light-Emitting Diodes. *J. Am. Chem. Soc.* **2021**, *143*, 1061-1068.
22. Zhang, B.; Wei, M.; Mao, H.; Pei, X.; Alshmimri, S. A.; Reimer, J. A.; Yaghi, O. M., Crystalline Dioxin-Linked Covalent Organic Frameworks from Irreversible Reactions. *J. Am. Chem. Soc.* **2018**, *140*, 12715-12719.
23. Guan, X.; Li, H.; Ma, Y.; Xue, M.; Fang, Q.; Yan, Y.; Valtchev, V.; Qiu, S., Chemically stable polyarylether-based covalent organic frameworks. *Nat. Chem.* **2019**, *11*, 587-594.
24. Yang, C.; Jiang, K.; Zheng, Q.; Li, X.; Mao, H.; Zhong, W.; Chen, C.; Sun, B.; Zheng, H.; Zhuang, X.; Reimer, J. A.; Liu, Y.; Zhang, J., Chemically Stable Polyarylether-Based Metallophthalocyanine Frameworks with High Carrier Mobilities for Capacitive Energy Storage. *J. Am. Chem. Soc.* **2021**, *143*, 17701-17707.
25. Waller, P. J.; Lyle, S. J.; Osborn Popp, T. M.; Diercks, C. S.; Reimer, J. A.; Yaghi, O. M., Chemical Conversion of Linkages in Covalent Organic Frameworks. *J. Am. Chem. Soc.* **2016**, *138*, 15519-15522.
26. Wang, Y.; Liu, H.; Pan, Q.; Wu, C.; Hao, W.; Xu, J.; Chen, R.; Liu, J.; Li, Z.; Zhao, Y., Construction of Fully Conjugated Covalent Organic Frameworks via Facile Linkage Conversion for Efficient Photoenzymatic Catalysis. *J. Am. Chem. Soc.* **2020**, *142*, 5958-5963.
27. Zhou, Z.-B.; Han, X.-H.; Qi, Q.-Y.; Gan, S.-X.; Ma, D.-L.; Zhao, X., A Facile, Efficient, and General Synthetic Method to Amide-Linked Covalent Organic Frameworks. *J. Am. Chem. Soc.* **2022**.
28. Zhang, M.; Li, Y.; Yuan, W.; Guo, X.; Bai, C.; Zou, Y.; Long, H.; Qi, Y.; Li, S.; Tao, G.; Xia, C.; Ma, L., Construction of Flexible Amine-linked Covalent Organic Frameworks by Catalysis and Reduction of Formic Acid via the Eschweiler–Clarke Reaction. *Angew. Chem. Int. Ed.* **2021**, *60*, 12396-12405.
29. Grunenberg, L.; Savasci, G.; Terban, M. W.; Duppel, V.; Moudrakovski, I.; Etter, M.; Dinnebier, R. E.; Ochsenfeld, C.; Lotsch, B. V., Amine-Linked Covalent Organic Frameworks as a Platform for Postsynthetic Structure Interconversion and Pore-Wall Modification. *J. Am. Chem. Soc.* **2021**, *143*, 3430-3438.
30. Liu, H.; Chu, J.; Yin, Z.; Cai, X.; Zhuang, L.; Deng, H., Covalent Organic Frameworks Linked by Amine Bonding for Concerted Electrochemical Reduction of CO2. *Chem* **2018**, *4*, 1696-1709.
31. Li, X.; Zhang, C.; Cai, S.; Lei, X.; Altoe, V.; Hong, F.; Urban, J. J.; Ciston, J.; Chan, E. M.; Liu, Y., Facile transformation of imine covalent organic frameworks into ultrastable crystalline porous aromatic frameworks. *Nat. Commun* **2018**, *9*, 2998.

32. Li, X.-T.; Zou, J.; Wang, T.-H.; Ma, H.-C.; Chen, G.-J.; Dong, Y.-B., Construction of Covalent Organic Frameworks via Three-Component One-Pot Strecker and Povarov Reactions. *J. Am. Chem. Soc.* **2020**, *142*, 6521-6526.
33. Waller, P. J.; AlFaraj, Y. S.; Diercks, C. S.; Jarenwattananon, N. N.; Yaghi, O. M., Conversion of Imine to Oxazole and Thiazole Linkages in Covalent Organic Frameworks. *J. Am. Chem. Soc.* **2018**, *140*, 9099-9103.
34. Wang, K.; Jia, Z.; Bai, Y.; Wang, X.; Hodgkiss, S. E.; Chen, L.; Chong, S. Y.; Wang, X.; Yang, H.; Xu, Y.; Feng, F.; Ward, J. W.; Cooper, A. I., Synthesis of Stable Thiazole-Linked Covalent Organic Frameworks via a Multicomponent Reaction. *J. Am. Chem. Soc.* **2020**, *142*, 11131-11138.
35. Wei, P.-F.; Qi, M.-Z.; Wang, Z.-P.; Ding, S.-Y.; Yu, W.; Liu, Q.; Wang, L.-K.; Wang, H.-Z.; An, W.-K.; Wang, W., Benzoxazole-Linked Ultrastable Covalent Organic Frameworks for Photocatalysis. *J. Am. Chem. Soc.* **2018**, *140*, 4623-4631.
36. Haase, F.; Troschke, E.; Savasci, G.; Banerjee, T.; Duppel, V.; Dörfler, S.; Grundei, M. M. J.; Burow, A. M.; Ochsenfeld, C.; Kaskel, S.; Lotsch, B. V., Topochemical conversion of an imine- into a thiazole-linked covalent organic framework enabling real structure analysis. *Nat. Commun* **2018**, *9*, 2600.
37. Majgier-Baranowska, H.; Williams, J. D.; Li, B.; Peet, N. P., Studies on the mechanism of the Cadogan–Sundberg indole synthesis. *Tetrahedron Lett.* **2012**, *53*, 4785-4788.
38. Genung, N. E.; Wei, L.; Aspnes, G. E., Regioselective Synthesis of 2H-Indazoles Using a Mild, One-Pot Condensation–Cadogan Reductive Cyclization. *Org. Lett.* **2014**, *16*, 3114-3117.
39. Creencia, E. C.; Kosaka, M.; Muramatsu, T.; Kobayashi, M.; Iizuka, T.; Horaguchi, T., Microwave-assisted Cadogan reaction for the synthesis of 2-aryl-2H-indazoles, 2-aryl-1H-benzimidazoles, 2-carbonylindoles, carbazole, and phenazine. *J. Heterocycl. Chem.* **2009**, *46*, 1309-1317.
40. Li, X.; Chu, S.; Feher, V. A.; Khalili, M.; Nie, Z.; Margosiak, S.; Nikulin, V.; Levin, J.; Sprankle, K. G.; Tedder, M. E.; Almassy, R.; Appelt, K.; Yager, K. M., Structure-Based Design, Synthesis, and Antimicrobial Activity of Indazole-Derived SAH/MTA Nucleosidase Inhibitors. *Journal of Medicinal Chemistry* **2003**, *46*, 5663-5673.
41. De Lena, M.; Lorusso, V.; Latorre, A.; Fanizza, G.; Gargano, G.; Caporusso, L.; Guida, M.; Catino, A.; Crucitta, E.; Sambiasi, D.; Mazzei, A., Paclitaxel, cisplatin and lonidamine in advanced ovarian cancer. A phase II study. *European Journal of Cancer* **2001**, *37*, 364-368.
42. Shen, H.; Gou, S.; Shen, J.; Zhu, Y.; Zhang, Y.; Chen, X., Synthesis and biological evaluations of novel bendazac lysine analogues as potent anticataract agents. *Bioorganic & Medicinal Chemistry Letters* **2010**, *20*, 2115-2118.
43. Sun, J.-H.; Teleha, C. A.; Yan, J.-S.; Rodgers, J. D.; Nugiel, D. A., Efficient Synthesis of 5-(Bromomethyl)- and 5-(Aminomethyl)-1-THP-Indazole. *The Journal of Organic Chemistry* **1997**, *62*, 5627-5629.
44. Cadogan, J. I. G.; Marshall, R.; Smith, D. M.; Todd, M. J., Reduction of nitro- and nitroso-compounds by tervalent phosphorus reagents. Part VIII. Syntheses of benzimidazoles and anthranils. *Journal of the Chemical Society C: Organic* **1970**, 2441-2443.
45. Kandambeth, S.; Mallick, A.; Lukose, B.; Mane, M. V.; Heine, T.; Banerjee, R., Construction of Crystalline 2D Covalent Organic Frameworks with Remarkable Chemical (Acid/Base) Stability via a Combined Reversible and Irreversible Route. *J. Am. Chem. Soc.* **2012**, *134*, 19524-19527.
46. Halder, A.; Karak, S.; Addicoat, M.; Bera, S.; Chakraborty, A.; Kunjattu, S. H.; Pachfule, P.; Heine, T.; Banerjee, R., Ultrastable Imine-Based Covalent Organic Frameworks for Sulfuric Acid Recovery: An Effect of Interlayer Hydrogen Bonding. *Angew. Chem. Int. Ed.* **2018**, *57*, 5797-5802.
47. Guo, Z.-C.; Shi, Z.-Q.; Wang, X.-Y.; Li, Z.-F.; Li, G., Proton conductive covalent organic frameworks. *Coord. Chem. Rev.* **2020**, *422*, 213465.
48. Chandra, S.; Kundu, T.; Kandambeth, S.; BabaRao, R.; Marathe, Y.; Kunjir, S. M.; Banerjee, R., Phosphoric Acid Loaded Azo (−N═N−) Based Covalent Organic Framework for Proton Conduction. *J. Am. Chem. Soc.* **2014**, *136*, 6570-6573.

49. Shinde, D. B.; Aiyappa, H. B.; Bhadra, M.; Biswal, B. P.; Wadge, P.; Kandambeth, S.; Garai, B.; Kundu, T.; Kurungot, S.; Banerjee, R., A mechanochemically synthesized covalent organic framework as a proton-conducting solid electrolyte. *J. Mater. Chem. A* **2016**, *4*, 2682-2690.
50. Xu, H.; Tao, S.; Jiang, D., Proton conduction in crystalline and porous covalent organic frameworks. *Nat. Mater.* **2016**, *15*, 722-726.
51. Tao, S.; Zhai, L.; Dinga Wonanke, A. D.; Addicoat, M. A.; Jiang, Q.; Jiang, D., Confining H3PO4 network in covalent organic frameworks enables proton super flow. *Nat. Commun* **2020**, *11*, 1981.
52. Ranjeesh, K. C.; Illathvalappil, R.; Veer, S. D.; Peter, J.; Wakchaure, V. C.; Goudappagouda; Raj, K. V.; Kurungot, S.; Babu, S. S., Imidazole-Linked Crystalline Two-Dimensional Polymer with Ultrahigh Proton-Conductivity. *J. Am. Chem. Soc.* **2019**, *141*, 14950-14954.
53. Yang, Y.; He, X.; Zhang, P.; Andaloussi, Y. H.; Zhang, H.; Jiang, Z.; Chen, Y.; Ma, S.; Cheng, P.; Zhang, Z., Combined Intrinsic and Extrinsic Proton Conduction in Robust Covalent Organic Frameworks for Hydrogen Fuel Cell Applications. *Angew. Chem. Int. Ed.* **2020**, *59*, 3678-3684.
54. Agmon, N., The Grotthuss mechanism. *Chem. Phys. Lett.* **1995**, *244*, 456-462.
55. Sasmal, H. S.; Aiyappa, H. B.; Bhange, S. N.; Karak, S.; Halder, A.; Kurungot, S.; Banerjee, R., Superprotonic Conductivity in Flexible Porous Covalent Organic Framework Membranes. *Angew. Chem. Int. Ed.* **2018**, *57*, 10894-10898.

Table of content graphic